

Article

Spatial and Temporal Characteristics of High-Temperature Heat Wave Disasters in Chongqing

Haijing Huang ^{1,2,*}, Pengyu Jie ¹, Yufei Yang ¹ and Shaoying Mi ³¹ School of Architecture and Urban Planning, Chongqing University, Chongqing 400030, China² Key Laboratory of New Technology for Construction of Cities in Mountain Area, Chongqing 400030, China³ Pioneer Architects, Panyu, Guangzhou 511400, China

* Correspondence: cqhhj@cqu.edu.cn

Abstract: In the background of global warming, heat wave disasters have become more frequent globally, and mountainous cities are more seriously affected by heat wave disasters due to the special features of topography and urban morphology. This paper analyzes the temporal and spatial distribution characteristics of heat wave disasters in Chongqing, a mountainous city. The results shows that heat wave disasters in Chongqing tend to increase overall and decrease locally before increasing. Significant growth in heat waves since 2010 and time series model prediction analysis shows that Chongqing will face more severe heat waves in the future. The spatial distribution of heat wave disasters varies significantly, high in the middle and low at the ends. There is a tendency for the center of heat wave disasters to shift from the south-central part of Chongqing to the northeast. In addition to the influence of atmospheric circulation and mountain topography, the causes are also positively related to urban development intensity and urbanization trends. It is necessary to develop specific control and management measures for heat waves depending on the characteristics of them. The take-home message of the study is the spatial and temporal trends of heat waves in Chongqing to provide a theoretical basis for high-temperature mitigation.

Keywords: high-temperature heat waves; Chongqing; spatial and temporal characteristics; influencing factors



Citation: Huang, H.; Jie, P.; Yang, Y.; Mi, S. Spatial and Temporal Characteristics of High-Temperature Heat Wave Disasters in Chongqing. *Atmosphere* **2022**, *13*, 1396. <https://doi.org/10.3390/atmos13091396>

Academic Editors: Sen Chiao, Robert Pasken, Ricardo Sakai and Belay Demoz

Received: 20 July 2022

Accepted: 27 August 2022

Published: 30 August 2022

Publisher's Note: MDPI stays neutral with regard to jurisdictional claims in published maps and institutional affiliations.



Copyright: © 2022 by the authors. Licensee MDPI, Basel, Switzerland. This article is an open access article distributed under the terms and conditions of the Creative Commons Attribution (CC BY) license (<https://creativecommons.org/licenses/by/4.0/>).

1. Introduction

In recent years, there has been continued evidence that the Earth's surface temperature is showing a long-term increase. The latest Sixth Assessment Report of the Intergovernmental Panel on Climate Change (IPCC), states that human-influenced global warming is responding to an increase in the frequency and intensity of extreme heat events, seawater warming, and heavy precipitation [1]. The World Meteorological Organization, WMO noted during the congress in June 2019 that temperatures in many parts of the world are at record highs again [2]. Among its latest statistical ranking of the impact of global natural disasters, extreme temperature impacts ranked fourth, after floods, storms, and earthquakes, before disasters such as landslides, droughts, and forest fires. High-temperature heat waves have become the most serious climate disasters in some countries [3,4], which are increasingly attracting attention to prevention and control of heat wave disasters [5,6].

High-temperature heat waves are weather processes with high temperature, high humidity, and long duration, making the human body feel uncomfortable, as well as potentially threatening public health and life safety, increasing energy consumption, and affecting social production activities [7]. Due to differences in geographical conditions and economic status, there is no uniform standard for measuring heat waves in different regions of the world, and in the process of conducting research on heat waves, researchers have defined and standardized heat waves differently. Heo et al. developed the human physiological equivalent temperature (PET) using the human heat wave equilibrium model, considering

PET > 41 °C as a heat wave warning criterion [8]. Aubrecht et al. defined a weather process with a duration of more than 3 days and a daily maximum temperature ≥ 30 °C as a high-temperature heat wave [9]. Heo et al. constructed a formula to calculate the heat index using temperature and relative humidity for classifying high-temperature heat waves [10]. To date, there is no universally accepted definition of a high-temperature heat wave. Most international organizations and developed countries generally define high-temperature heat waves in terms of two scales: maximum daily temperature and duration [11–14].

Research on high-temperature heat waves involves multidisciplinary research areas such as meteorology, disaster science, environmental science, urban planning, and medicine and health [15–18], while the research on the spatial and temporal characteristics of high-temperature heat wave disasters includes two levels: national and regional. At the national level, Chinese scholars studied the spatial and temporal characteristics of the intensity of heat waves (IHW), the frequency of heat waves (FHW), and the number of heat wave days (NHD) in China from 1961 to 2010 using daily maximum temperatures and related heat wave indicators from 753 stations nationwide. Meanwhile, it was found that the FHW, NHD, and IHW of high-temperature heat waves showed chronological characteristics, with a decreasing and then increasing trend from the 1960s to the 2010s [19]. Xinjiang and southeastern China are the two main regions with high frequency of extreme heat events [20]. When it comes to international research, Kuglitsch et al. [21] studied the temporal characteristics of high-temperature heat waves in the Mediterranean region by using data statistics from 246 meteorological stations in the eastern Mediterranean from 1961 to 2006, finding that the increase in IHW in Mediterranean countries was higher than previously reported; Xian-XiangLi studied the heat wave trends in Southeast Asian countries during 1979–2018 and noticed that heat waves are becoming more frequent and longer in most Southeast Asian countries [22]. Some researchers studied the spatial and temporal characteristics of high-temperature heat waves in Central European countries by comparing data differences between different regional climate models (RCMs) [23]. At the regional level, Chinese academics analyzed the spatial and temporal variation of heat waves in the Nanjing metropolitan area, China, discovering that factors such as impermeable substrates and highly reflective building materials accelerate the urban heat island (UHI) effect and interact with heat waves [24]. NHD in Chongqing, a high-density mountainous city, has an impact on factors like UHI [25]. NHD in different cities also affects health-related factors, including death rates [26]. Zhang, Kehui et al. [27] analyzed the data on NHD, FHW, and extremely high temperature in the Hebei region from 1956 to 2009, deriving the spatial and temporal distribution characteristics of high-temperature heat waves in the Hebei region. Chen Min et al. [14] defined the three-level criteria for heat waves in Shanghai and introduced the concept of “high-temperature effective accumulation temperature” to analyze the multiscale time-frequency characteristics of heat waves in the region. Zhou Yang et al. [28] obtained high spatial resolution of near-surface air temperature impact conditions by processing multisource remote sensing data in order to study the spatial distribution characteristics of heat wave disasters in Nanjing. There are also many international studies at this level. Dousset et al. [29] used remote sensing data to analyze the spatial and temporal variability of Paris land surface temperature (LST) and studied high-temperature heat waves in combination with physical properties of the land surface. Rachel E. S. Clemesha et al. [30] analyzed the spatial and temporal evolution of high-temperature heat waves in California based on coastal low cloudiness (CLC), a key factor of California’s summer coastal climate, which revealed that heat waves are unusually intense along the coast.

Under the background of the overlapping of climate change and the urbanization process, global warming combined with the characteristics of dense urban population with space and a high degree of economic integration has triggered urban heat waves. Mountain cities have more intense heat wave disasters and more complex changes due to their complex topography, special substrate environment, dense buildings, and concentrated population; however, the dynamic change characteristics of heat waves in mountain cities

and their influencing factors have been explored less from the perspective of temporal evolution and spatial distribution in the past [31]. Motivated by the above-mentioned knowledge gaps, this study is dedicated to exploring the spatial and temporal distribution characteristics of high-temperature heat waves in Chongqing in order to propose predictions and analyzing influencing factors based on research data. According to the overall objective, the specific objectives of this study are: (1) through statistical analysis of meteorological station data to summarize the trend of FHW, NHD, and IHW over time in Chongqing from 1959 to 2020; (2) to analyze the differences in the spatial distribution of high-temperature heat waves in different regions of Chongqing; (3) to analyze the sub-surface type and urbanization level of each region in Chongqing and, combined with the spatial distribution of high-temperature heat waves, derive the influencing factors of high-temperature heat waves in Chongqing. Overall, it provides a basis for disaster risk prevention and control strategy development.

2. Materials and Methods

2.1. Research Area

Chongqing is one of the four “stove” cities in China (the four largest Chinese cities with the hottest summer weather), with a city area of 82,402 square kilometers, located between 105°11′–110°11′ East longitude and 28°10′–32°13′ North latitude, in the upper reaches of the Yangtze River. Around the city there are mountains such as Daba Mountain, Wuling Mountain, Wushan Mountain, and Dalou Mountain, the terrain is mainly hilly and mountainous. The climate is subtropical monsoon, with hot and dry summers and uneven rainfall. The average annual rainfall is abundant, and the average rainfall by season is 315 mm in spring, 488 mm in summer, 318 mm in autumn, and 69 mm in winter, with precipitation mostly concentrated in May–September, accounting for about 70% of the total annual precipitation. The average annual relative humidity is mostly 70–80%, which belongs to the high humidity area in China. According to Köppen climate classification rules, Chongqing belongs to type Cfa (humid subtropical climate). July and August are the sunniest months of the year, with sunshine hours accounting for about 40% of the year. Long hours and high intensity of solar radiation are the direct cause of the formation of high-temperature heat waves in Chongqing.

2.2. Data and Source

The data of 12 meteorological observation stations (including 1 national benchmark climate station and 11 national basic meteorological stations) in Chongqing provided by the National Meteorological Science Data Center of China were selected as data sources. In order to ensure the consistency and coherence of the meteorological data, the starting time of the meteorological station data records was sorted out, determining 1959 as the starting time and 2020 as the cut-off time for the latest start of records among the 12 stations. According to the definition of high-temperature heat waves by the China Meteorological Administration, the meteorological data with daily maximum temperature greater than or equal to 35 °C and duration greater than or equal to 3 days from May to September 1959–2020 at 12 meteorological stations were programmed using VBA macro language for analysis (Figure 1, Table 1).

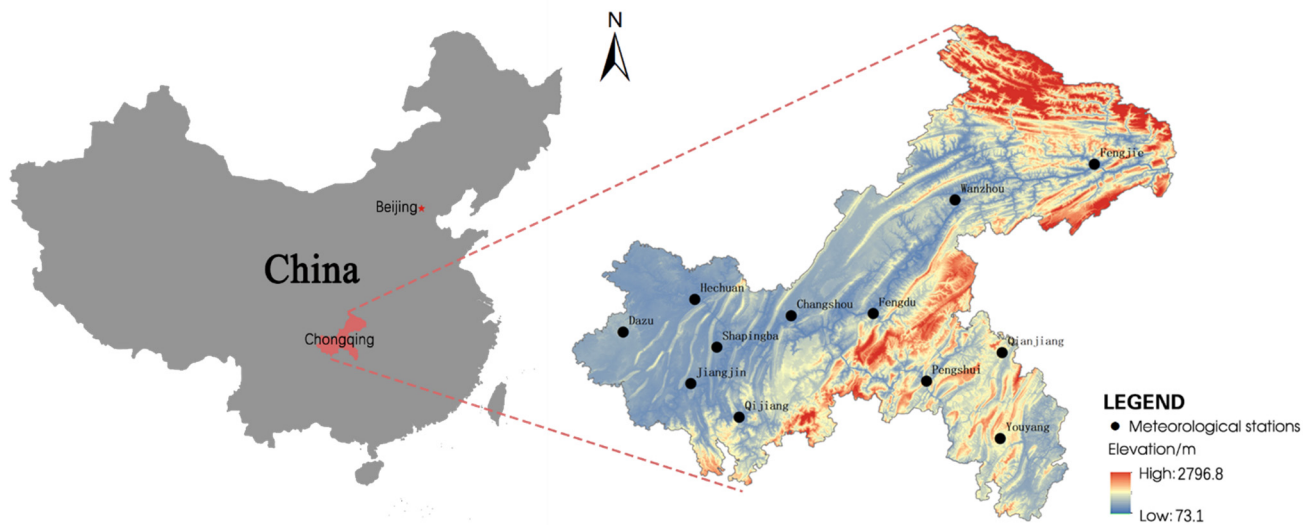


Figure 1. Location of Chongqing and Chongqing city elevation and meteorological station distribution (China Map Review Number: GS (2016) 1551).

Table 1. Basic information of 12 weather stations in Chongqing.

Meteorological Station Number	Name of Station	Latitude (°)	Longitude (°)	Elevation (m)	Data Start Date
57348	Fengjie	31.067	109.533	299.8	1954
57432	Wanzhou	30.776	108.400	186.7	1954
57502	Dazu	29.700	105.700	377.6	1957
57512	Hechuan	29.966	106.283	230.6	1959
57516	Shapingba	29.576	106.461	259.1	1951
57517	Jiangjin	29.280	106.25	261.4	1955
57520	Changshou	29.833	107.067	377.6	1959
57523	Fengdu	29.850	107.733	290.5	1959
57536	Qianjiang	29.533	108.783	607.3	1959
57537	Pengshui	29.300	108.167	322.2	1951
57612	Qijiang	29.006	106.643	254.8	1957
57633	Youyang	28.833	108.767	664.1	1951

2.3. Calculation and Statistical Analysis of High-Temperature Heat Wave Indicators

In this study, we analyze three key indicators of heat waves: FHW, NHD, and IHW. FHW refers to the average number of heat waves (d/a: “d” is the number of days and “a” is the annual) at a site in a given year. NHD is the average number of accumulated days of heat waves (d/a) at a site in a given year. IHW is calculated using the concept of effective accumulated high temperature (EAHT), which refers to the annual average (°C-d/a) of the cumulative values of daily maximum temperatures above the heat wave threshold (35 °C) during a heat wave at a station. For statistical and trend analysis of the above three heat waves data, the Mann–Kendall (M-K test has the characteristics of not being affected by sample values, distribution types, etc., and is recommended by the WMO and widely used) nonparametric rank order statistical test [32,33] was used to determine the local change trend and sudden change test for their time series; the details are as follows:

Let the original sequence be y_1, y_2, \dots, y_n , the i -th sample y_i is greater than y_j ($1 \leq j \leq i$) cumulatively denoted as m_i , and define the statistic:

$$d_k = \sum_{i=1}^k m_i, \quad (2 \leq k \leq n) \tag{1}$$

Assuming that the original series is random and independent, the mean of d_k is denoted by $E(d_k)$ and the variance by $var(d_k)$:

$$E(d_k) = k(k - 1)/4 \quad (2)$$

$$\text{Var}(d_k) = k(k - 1)(2k + 5)/72 (2 \leq k \leq n) \quad (3)$$

Standardizing d_k , we obtain:

$$UF_k = \frac{d_k - E(d_k)}{\sqrt{\text{Var}(d_k)}} (k = 1, 2, \dots, n) \quad (4)$$

UF_k in the above equation satisfies the standard normal distribution, and for a given significance level α , if $|UF_k| \geq U_\alpha$, it means that the sample has a significant change in trend. After arranging the samples in reverse order and recalculating them according to the above equation, UB_k is obtained, and UB_k satisfies:

$$\begin{cases} UB_k = -UB_k \\ k = n + 1 - k \end{cases} \quad (5)$$

UF_k and UB_k are plotted as UF and UB curves. If UF_k and UB_k intersect and the intersection point is within the confidence interval, the point may be a mutation point. If both UF_k and UB_k are greater than 0, it indicates that the time series is an upward trend; if both curves are less than 0, the time series is a downward trend. Given the significance level $\alpha = 0.05$, $U_{0.05} = \pm 1.9$, if both UF_k and UB_k exceed the critical value at the same time, it indicates that the time series is significantly rising or falling; at the significance level $\alpha = 0.01$, $U_{0.01} = \pm 2.56$, if both UF_k and UB_k exceed the critical value at the same time, it indicates that the time series is highly significantly rising or falling.

Then time series analysis in SPSS (IBM Company, version 26, from Chicago, IL, USA) was used to fit forecasts for the 3 indicators of heat waves with forecast years 2021–2030. ArcGIS Map software was used to map the spatial distribution of high-temperature heat waves to study the spatial distribution patterns and trends of historical heat waves in Chongqing, two methods were used: the ordinary Kriging interpolation method and the natural intermittent point grading method.

2.4. Analysis of Subsurface Types and Urbanization Levels in Chongqing

Focusing on the spatial and temporal characteristics of heat waves in Chongqing, in order to analyze the correlation between regional factors (subsurface types and urbanization levels) and heat waves, Globe Land 30 global land cover data were used to analyze the changes in subsurface types in Chongqing; according to the global night-time light remote sensing data from the Resource and Environment Science and Data Center of the Chinese Academy of Sciences, the changes of urbanization levels in Chongqing were analyzed. Since there is a break in the night-time light remote sensing data around 2013, DMSP data from 1992 to 2013, and visible infrared imaging radiometer suite (VIIRS) data after 2013, the two data cannot be converted and compared, so the night-time light defense meteorological satellite program (DMSP) data before 2013 are used for comparison in this study.

3. Results and Discussion

3.1. Temporal Variation Characteristics of Chongqing's High-Temperature Heat Waves

Comprehensive statistics of daily maximum temperature data from May to September at 12 meteorological stations in Chongqing from 1959 to 2020 show that the average FHW, NHD, and IHW in Chongqing over 62 years were 3.2 times/a, 20.2 d/a, and 46.7 °C·d/a. The average duration of a single high-temperature heat wave reached 6.3d, which was more than twice the 3d definition of a high-temperature heat wave by the China Meteorological Administration. The average temperature during a high-temperature heat wave reached 37.3 °C, which was 2.3 °C higher than the standard 35 °C for heat waves. In order to clearly show the global change characteristics of Chongqing high-temperature heat waves, the data from all meteorological stations were studied by taking the average value.

The changes in the average FHW of all meteorological station in Chongqing from 1959 to 2020 are shown in Figure 2a, with a range of 0.8–7.0 times/a and a variation interval

reaching 6.2 times/a, where the maximum value occurred in 2013 and the minimum value occurred in 1993. Overall, the FHW showed a slow upward trend (green line in Figure 2a), increasing at a growth rate of 0.0105 times/a.



Figure 2. Historical changes in the FHW in Chongqing from 1959 to 2020 and M-K test curves; (a) changes in FHW; (b) M-K test curves.

The changes in the average NHD of all meteorological stations in Chongqing from 1959 to 2020 are shown in Figure 3a, with a range of 3.2–46.2 d/a and a variation interval reaching 43.0 d/a, in which the maximum value appeared in 2006 and the minimum value appeared in 1993. Generally, the NHD showed an increasing trend (green line in Figure 3a), with a growth rate of 0.0921 d/a. Using the minimum standard of a three-day heat wave, the growth rate of the number of days was more than three times the growth rate of the frequency, indicating that the duration of a single heat wave was also increasing significantly.

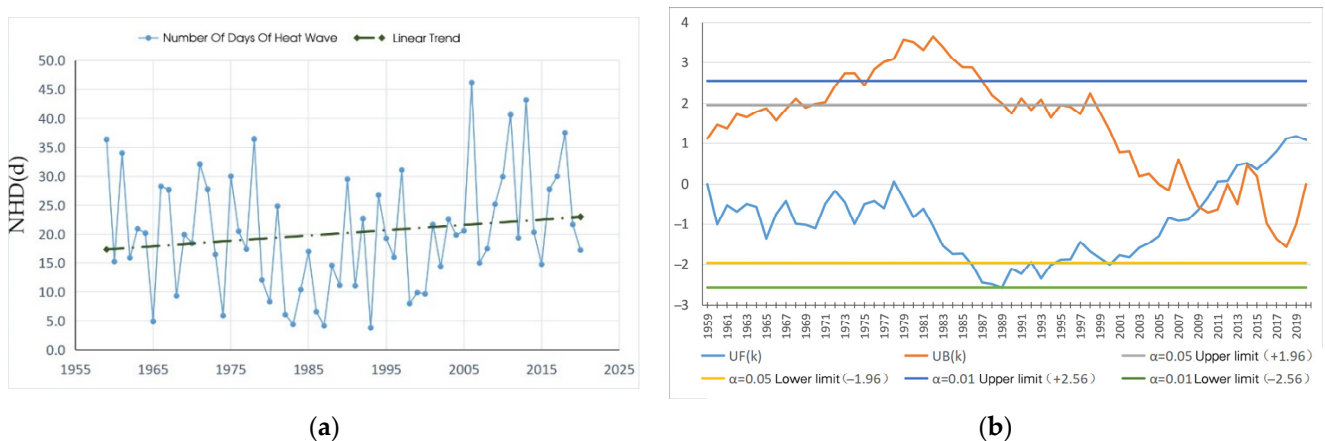


Figure 3. Historical changes in the NHD in Chongqing from 1959 to 2020 and M-K test curves; (a) changes in NHD; (b) M-K test curves.

The average IHW of all Chongqing meteorological stations from 1959 to 2020 varies as shown in Figure 4a, with a range of 4.3–46.2 °C·d/a and a variation interval reaching 41.9 °C·d/a, during which the maximum value happened in 2006 and the minimum value happened in 1987. On the whole, the IHW showed a significant increasing trend (green line in Figure 4a), with a growth rate of 0.4908 °C·d/a.

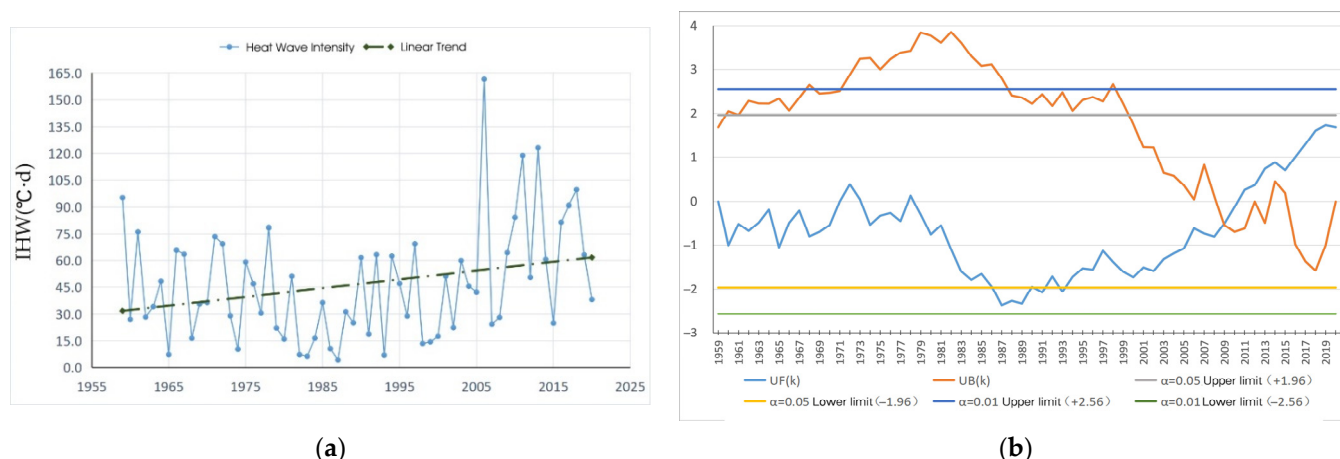


Figure 4. Historical changes in the IHW in Chongqing from 1959 to 2020 and M-K test curves; (a) changes in IHW; (b) M-K test curves.

For the further understanding of the local change characteristics and sudden change time points of the high-temperature heat waves in Chongqing, the M-K test was used to plot the trend curves, as shown in Figures 2b, 3b and 4b. In the figures, $UF(k)$ is the statistical series of the tested data calculated in time order, the positive or negative of its value can represent the temporal change trend of the tested data. $UB(k)$ is the statistical series calculated in time inverse sequence. Its value $UB(k) = -UF(k)$, ($k = n, n - 1, \dots, 1$). $U_{0.05} = \pm 1.9$ at the significance level $\alpha = 0.05$ and $U_{0.01} = \pm 2.56$ at the significance level $\alpha = 0.01$ given in the figure. When the $UF(k)$ curve is outside the range framed by the significance level straight line, it indicates a significant upward or downward trend at this stage. If the intersection of $UF(k)$ and $UB(k)$ curves occurs and the intersection point lies within the range framed by the significance level straight line, then the time corresponding to the intersection point is the time when the sudden change begins.

The M-K test curve trends of the FHW, NHD, and IHW in Chongqing have a strong consistency. Based on the change curve trends, the local changes of high-temperature heat waves in Chongqing were divided into three stages. The first stage (1959–1978) was the slow decreasing stage, the UF value in this stage was less than 0, but its curves were all distributed around the X-axis, which proves that the heat waves in this stage had a slow decreasing trend. The second stage (1978–2011) was the significant decreasing stage, the UF value in this stage decreased significantly, among which the UF value in 1986–1994 was even below the lower threshold of $\alpha = 0.05$. It indicates a significant decreasing trend of high-temperature heat waves in this stage. The third stage (2011–2020) was the growth stage, in which the UF value was greater than 0 and the growth rate was increasing, showing a significant growth trend of high-temperature heat waves in Chongqing in this stage. It can also be seen from the heat wave changes graph that the intersection points of its $UF(k)$ and $UB(k)$ curves were both located near 2009, with the intersection points all located within the range framed by the significance level straight line. It can be judged that the three data of heat waves in Chongqing city began to change suddenly near 2009.

In addition, to further verify the temporal variation characteristics of the FHW, NHD, and IHW in Chongqing and to make certain predictions on the future development trend of high-temperature heat waves in Chongqing on the basis of verifying the measured data, three indicators were firstly analyzed by the ARIMA model analysis in time series analysis, and the stability analysis was firstly conducted according to the selected conditions of autocorrelation figure (ACF) and partial autocorrelation figure (PACF), repeatedly verified. The autoregressive (p), differential (d), and moving average (q) of the three indicators were determined, followed by model construction with NHD (13,1,7), FHW (13,1,5), and IHW (10,1,4). After fitting analysis, the fitted prediction graphs (Figure 5) of the three indicators and the prediction table of heat wave indicators (Table 2) for the decade of 2021–2030

were obtained, and it can be seen that all three indicators fit well. Furthermore, the trend of the fitted data was similar to the measured data, showing a slow decline followed by a rising trend. The predicted curve after 2020 showed a significant increase, which was consistent with the rising trend after 2010. As to the predicted average values for the decade of 2020–2030, NHD (37.0 d), FHW (5.1 times), and IHW (108.3 °C·d) were higher than the average values of indicators in any decade during 1959–2020. It can be predicted that heat waves in Chongqing will become increasingly severe in the future.

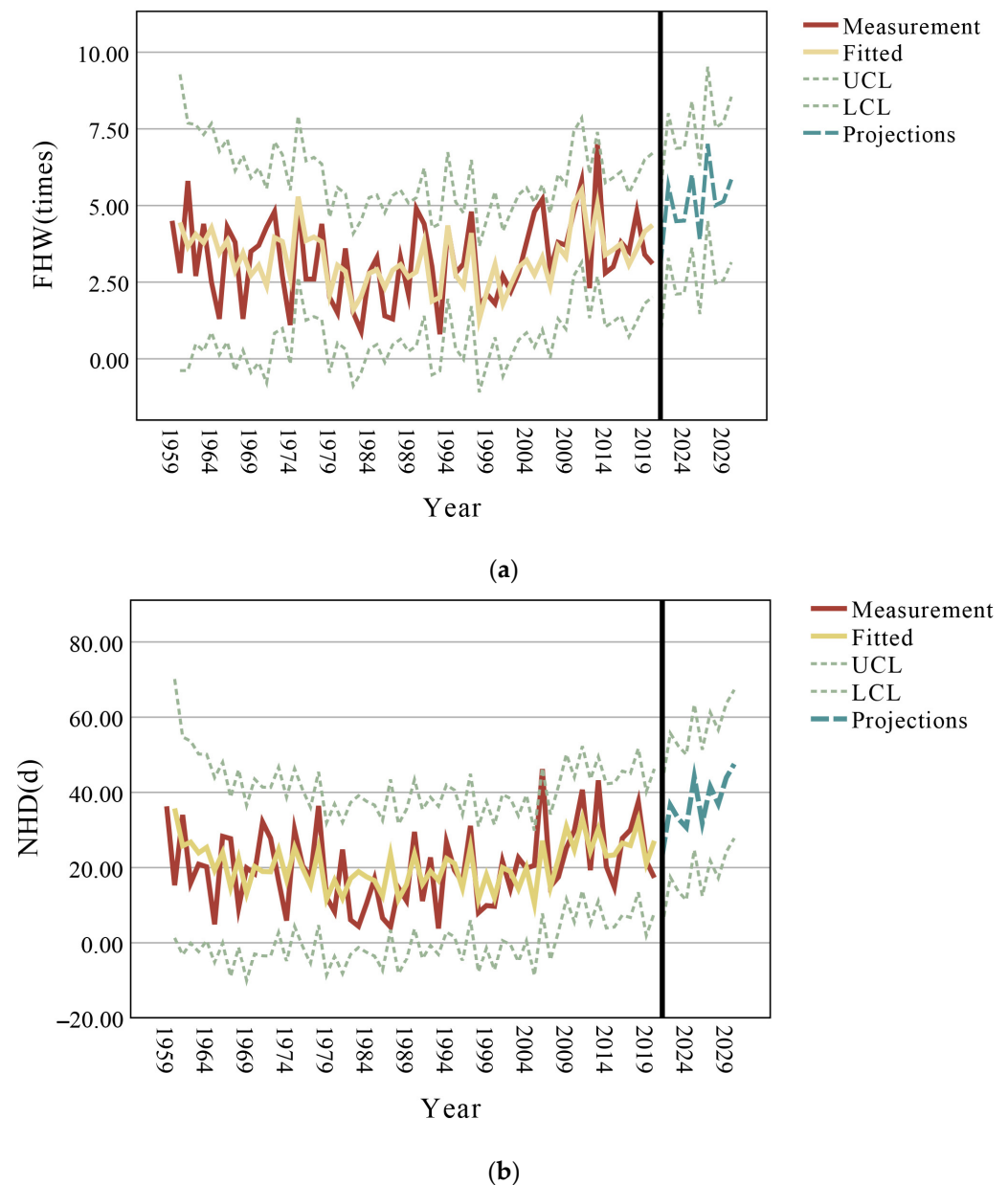


Figure 5. Cont.

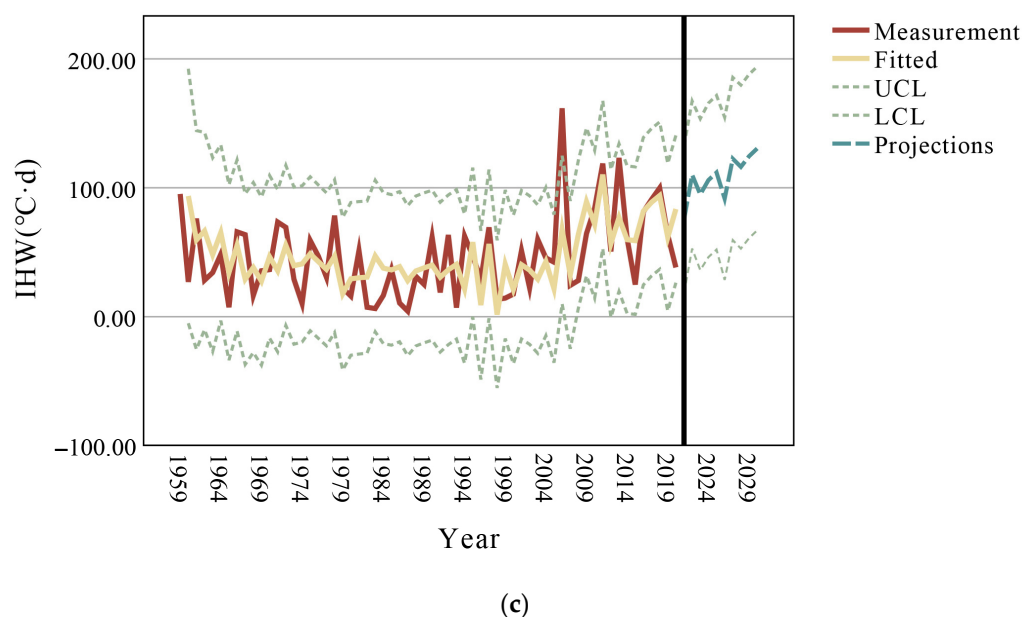


Figure 5. Fitted forecast graph of Chongqing’s high-temperature heat waves; (a) FHW fitted prediction graph; (b) NHD fitted prediction graph; (c) IHW fitted prediction graph.

Table 2. ARIMA model prediction table.

		2021	2022	2023	2024	2025	2026	2027	2028	2029	2030
Average IHW prediction model	Prediction	75.34	110.06	94.84	105.91	111.84	91.58	122.51	116.24	124.44	130.48
	UCL	132.49	167.27	153.56	165.65	171.61	154.62	185.59	179.65	187.96	194.00
	LCL	18.19	52.85	36.11	46.17	52.07	28.54	59.43	52.82	60.92	66.95
Average NHD prediction model	Prediction	23.45	36.60	33.01	30.70	44.05	31.90	41.53	36.92	43.89	47.54
	UCL	42.58	55.73	52.36	50.06	63.39	51.34	61.26	56.61	63.60	67.28
	LCL	4.32	17.47	13.66	11.34	24.71	12.45	21.80	17.22	24.18	27.79
Average FHW prediction model	Prediction	3.01	5.65	4.49	4.51	6.01	3.88	7.01	5.01	5.13	5.85
	UCL	5.35	8.01	6.86	6.88	8.40	6.29	9.53	7.54	7.71	8.55
	LCL	0.67	3.29	2.11	2.13	3.62	1.46	4.50	2.47	2.56	3.15

A comprehensive analysis of the temporal change pattern of the FHW, NHD, and IHW in Chongqing from 1959 to 2020 showed that the changing trend of the three key indicators was highly consistent, with an overall increasing trend of higher and higher frequency, more and more days, and more intense heat waves. There was a trend of decreasing and then increasing in stages, especially since the 2010s when the three indicators increased significantly. It can be judged combining the time series analysis model that the risk of high-temperature heat wave disasters faced by Chongqing in the future will remain very severe. This conclusion is consistent with the changes in heat waves in China over the decades [34], with significant temperature increases over 40 years in Chongqing, which is about 1.6 times warmer than the global warming trend [25]. The FHW, NHD, and IHW of heat waves in Chongqing are the largest among the 31 cities studied [35]

3.2. Spatial Distribution Characteristics of High-Temperature Heat Waves in Chongqing

Comparing the average FHW, NHD, and IHW at 12 meteorological stations in Chongqing, the station with the highest FHW was Qijiang, with 4.8 times/a, 1.50 times the average frequency in Chongqing. The station with the highest NHD was Wanzhou, reaching 31.6 d/a, 1.56 times the average number of days in Chongqing. The station with the highest IHW

was Fengdu, achieving 82.2 °C-d/a, which is 1.76 times of the average value in Chongqing. Among the three statistics of all meteorological stations, Youyang station was the lowest, with the FHW, NHD, and IHW only 0.2 times/a, 0.7d/a, and 0.6 °C-d/a respectively, which are only 6.25%, 3.47% and 1.28% of the average value of Chongqing city.

By using the spatial interpolation tool of ArcGIS Map software, the three indicators of high-temperature heat waves at each meteorological station in Chongqing were spatially interpolated. The data weights of different locations in the overall space were calculated by the distance between each meteorological observation point and the overall spatial arrangement to derive a continuous spatial distribution map of high-temperature heat waves, as shown in Figure 6. The spatial performance of the average FHW, NHD, and IHW tended to be consistent among the stations, all showing a distribution with a high middle and low sides. The area with the most severe heat wave disaster was located in central Chongqing, where the FHW, NHD, and IHW at Wanzhou and Fengdu sites were in the first rank. The southwest region was second only to the central part of the heat waves serious area, this region contains Jiangjin, Qijiang, and other districts. The regions least affected by heat waves were located in southeastern Chongqing, where two Youyang and Qianjiang sites were much lower than other regions in terms of three indicators values.

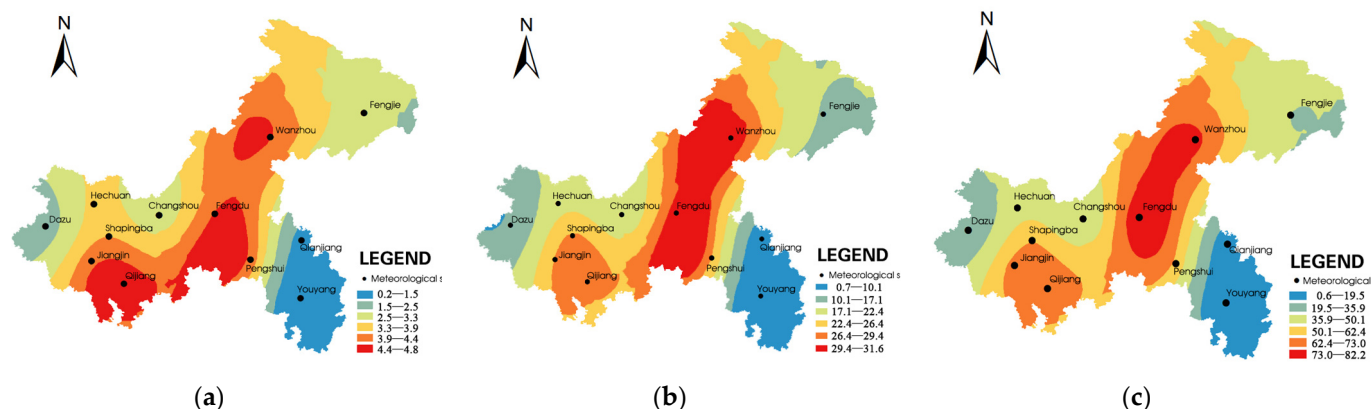


Figure 6. Spatial distribution of the average FHW, NHD, and IHW at each meteorological station in Chongqing; (a) spatial distribution of FHW; (b) spatial distribution of NHD; (c) spatial distribution of IHW.

3.3. Interdecadal Spatial Trends of High-Temperature Heat Waves in Chongqing

To explore the trend changes in the spatial distribution of high-temperature heat waves in Chongqing, this paper divides the heat wave characteristics data from meteorological stations in Chongqing into six interdecadal periods of 60s, 70s, 80s, 90s, 00s, and 10s and uses ArcGIS software to spatially interpolate the interdecadal averages of three key indicators of heat waves for each interdecadal period. This results in a spatial distribution diagram of the FHW, NHD, and IHW for each interdecadal period (Figure 6). Since the natural intermittent point method is graded each time based on the special situation of its own indicators, the plots are not comparable with each other. In order to increase the comparability between different interdecadal periods, the indicator scales of the FHW, NHD, and IHW spatial distribution maps of different interdecadal periods are re-graded in Figure 7 (Figure 6 scale is the scale generated by the natural intermittent point method), which makes the color between each interdecadal period represented by the indicator values the same between each interdecadal period, allowing for easy map reading and comparison.

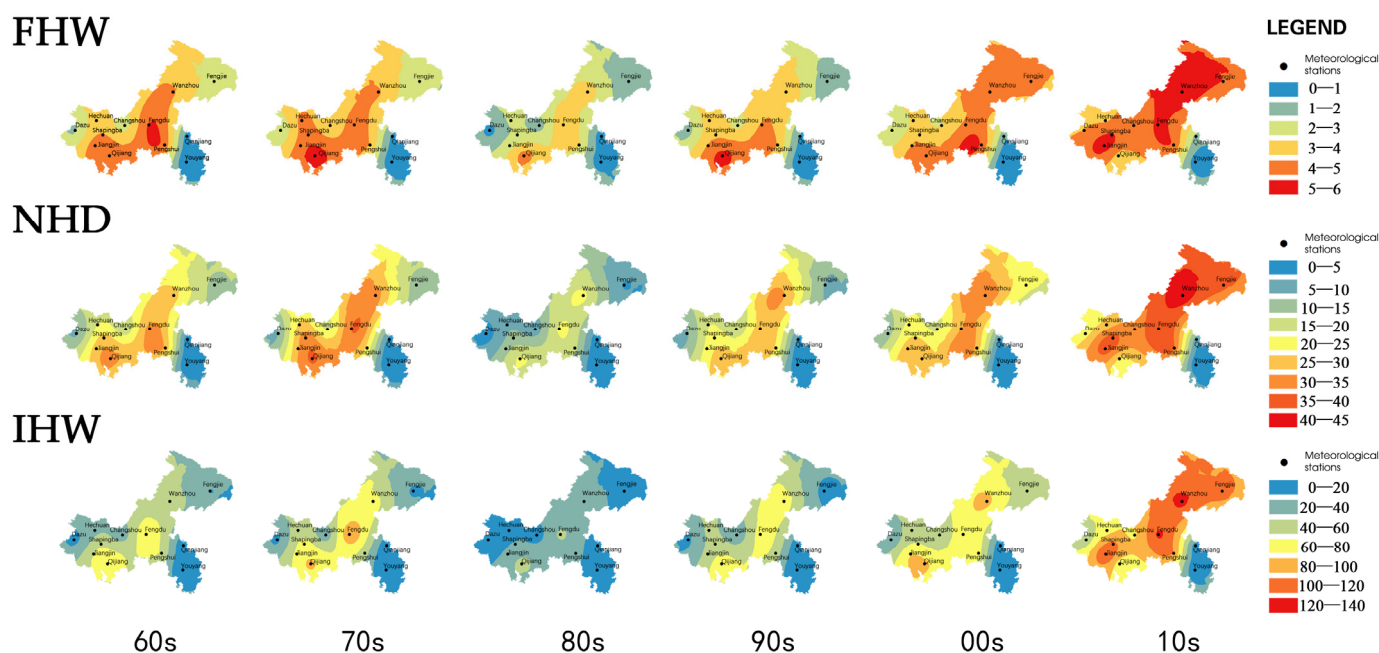


Figure 7. Spatial distribution of FHW, NHD, and IHW of interdecadal high-temperature heat waves at various meteorological stations in Chongqing.

It is shown in Figure 7 that the interdecade spatial trends of the three heat wave indicators in Chongqing had strong consistency. During the period from the 1960s to the 2010s, the 1980s was the era with the lowest heat wave impact. Meanwhile, the nearest 2010s was the era with the most severe heat wave disaster, with a significant increase in the heat wave level and an obvious expansion of the impact area. The central area of heat wave disasters showed a trend of shifting from the south-central to the northeastern part of Chongqing. From the 1960s to 1970s, the most severe heat wave areas in Chongqing were Fengdu, Pengshui, Qijiang, and other areas in the south-central part of Chongqing. In 2010s, the center of heat waves was Wanzhou (Wanxian was renamed Wanzhou District in 1998 and became the second largest city in Chongqing in 2010) and its surrounding areas, which obviously shifted to the northeast. The areas least affected by heat waves are always located in Youyang and Qianjiang in southeastern Chongqing (remote mountainous areas with slower development), without much interdecadal variability and significant spatial variation. Related studies have also shown significant interdecadal differences in heat waves in China after the 1990s, with a significant increase in the spatial distribution of heat waves over the next two decades [36]. Notable are the frequency, intensity, and duration of extreme high temperatures in the southwest [37], further validating the interdecadal trend of high-temperature heat waves in Chongqing.

3.4. Factors Influencing the Heat Waves in Chongqing

The causes of the spatial and temporal patterns of the FHW, NHD, and IHW in Chongqing are more complicated. Combining relevant studies and scientific analyses at home and abroad, it is concluded that there are two main influencing factors. Firstly, regional natural factors, including atmospheric circulation conditions, topography and topography, wind speed and direction [38,39]. Secondly, urban artificial factors, including urban spatial structure, subsurface types, and urbanization levels [40,41].

General circulation conditions, latitude, altitude, and mountain range orientation of the region in which the city is located are the most important factors affecting the climate of mountainous cities [42]. It has been shown that the Chongqing area is influenced by the eastward movement of the western Pacific subpressure and the westward extension of the South Asian high pressure, forming a superposition of upper and lower high-pressure situation. The prevalence of sinking airflow and suppressed convective activity are impor-

tant reasons for the persistent high temperature in Chongqing area [43,44]. Meanwhile, as seen in Figures 1 and 5, the severe heat wave area in Chongqing has a high overlap with the Yangtze River valley under the enclosure of the Daba Mountain Range and the Wuling Mountain Range, where the spatial distribution of high-temperature heat waves is significantly influenced by the slowing down and shading effects of the mountainous topography on wind speed and direction.

There are strong correlations between the spatial and temporal distribution of high-temperature heat waves and the types of subsurface and urbanization levels. It has been found that mountainous cities exacerbate the effects of high-temperature heat waves due to higher urban surface roughness (USR) and building density, which affects their ventilation efficiency [45] and increases the surface temperature. Mountain cities have an undulating and rough subsurface, which leads to less wind speed and not easily dissipating heat, exacerbating the impact of high-temperature heat waves. From Figure 8, it can be observed that the subsurface types in areas with intense heat wave disasters, such as the main city of Chongqing and Wanzhou district, were mostly artificial surfaces, and their artificial surface areas increased from 0.70% in 2000 to 3.20% in 2020. Meanwhile, the subsurface types in the southeast are mostly green cover, with weaker heat wave effects. The night-time light remote sensing data in Figure 9 can characterize the urbanization level and intensity of human activities in this region. It is known from the data changes in Figures 7 and 9 that the intensity of high-temperature heat wave disasters was positively correlated with the urbanization level in the region, and the higher the urbanization level (e.g., main urban area, Wanzhou district, etc.), the more intense the impact of high-temperature heat wave disasters. Related research has also shown that urbanization factors such as an urban lake area, high-rise high-density urban form, and the percentage of urban ecological land (UEL) can lead to an enhanced UHI effect and thus exacerbate high-temperature heat waves [46,47]. Appropriate urban form planning can improve urban climate resilience [48], thus contributing to the mitigation of heat waves [49]. This indicates the importance of urbanization factors for heat wave mitigation.

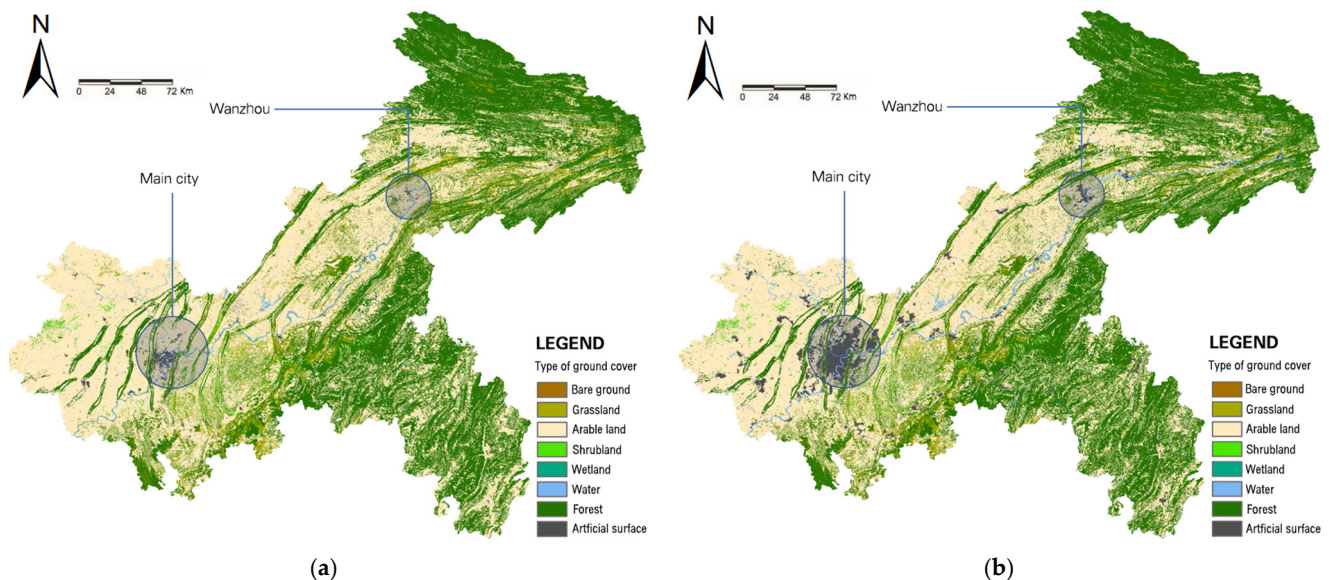


Figure 8. Changes in surface cover types in Chongqing; (a) type of surface cover in 2000; (b) type of surface cover in 2020.

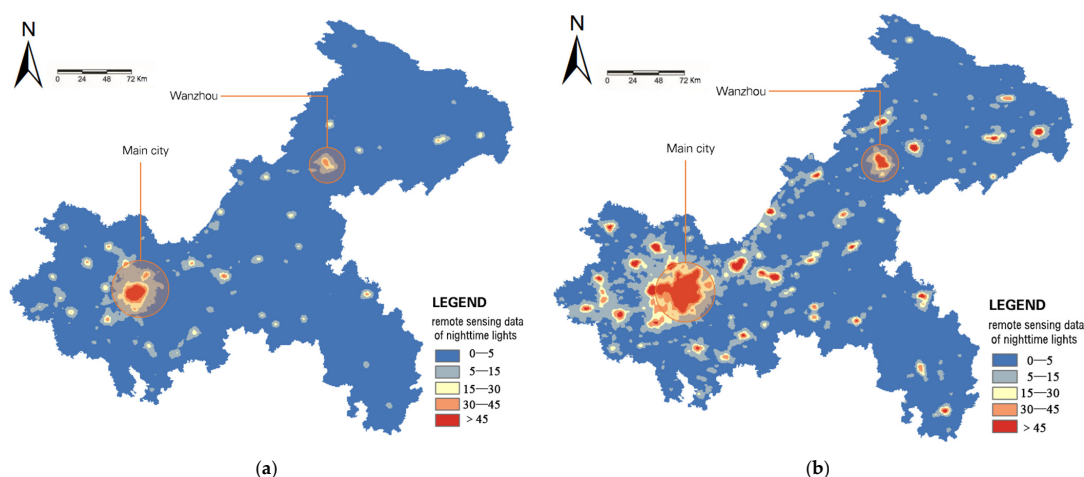


Figure 9. Changes in remote sensing data of night-time lights in Chongqing; (a) remote sensing of night lights in 2000; (b) remote sensing of night lights in 2020.

4. Conclusions and Implications

Through statistical analysis of daily maximum temperatures at 12 meteorological stations in Chongqing from 1959 to 2020, we summarized the characteristics of the spatial and temporal distribution of the FHW, NHD, and IHW in Chongqing and the influencing factors. Initially, the temporal change pattern and spatial distribution differences of high-temperature heat waves in Chongqing were revealed. Moreover, we made some judgments on the future development trend of high-temperature heat waves based on the research results. The main conclusions are as follows.

(1) The temporal trends of the FHW, NHD, and IHW in Chongqing from 1959 to 2020 were relatively consistent, with an overall increasing trend and a local trend of first decreasing and then increasing. In particular, the decreasing trend of FHW, NHD, and IHW in Chongqing was most obvious in the 1980s. After 2010, these three data increased significantly again. The inflection point for sudden changes in heat wave disasters in Chongqing occurred near 2009. The ARIMA time series model prediction results showed that the heat waves in Chongqing will continue to show a significant upward trend after 2020, and the risk of heat waves in Chongqing is very serious.

(2) The spatial distribution of high-temperature heat wave disasters in Chongqing from 1959 to 2020 varied significantly. Regions with the most severe heat wave disasters are located in central and southwestern Chongqing (the main urban area and Wanzhou, Fengdu, Qijiang, and other districts and counties), while regions least affected by heat waves are located in southeastern Chongqing (Youyang, Qianjiang, and other districts and counties), where the FHW, NHD, and IHW are much lower than those of other regions.

(3) In Chongqing from 1959 to 2020s the level of high-temperature heat wave disasters increased significantly, and the impact area was expanded. Up to the decade and twenties of the 21st century, the area affected by high-grade and high-intensity heat wave disasters significantly increased. Meanwhile, the center of high-temperature heat waves also shifted from Fengdu and Qijiang in the south-central part of the 1960s and 1970s to Wanzhou and the surrounding areas in the northeast where urban development was faster.

(4) Spatial and temporal characteristics and trends of high-temperature heat waves in Chongqing are influenced by regional natural factors such as global atmospheric circulation changes, topography, wind speed and direction, and are closely related to urban artificial factors such as urban space structure, subsurface types, and urbanization levels.

High-temperature heat waves are one of the sudden disasters faced by the global community, presenting an increasingly serious trend. On one hand, it is necessary to control the scale of cities, organize urban structures and ventilation corridors, reduce hard surfaces, and increase greenery to reduce the aggravating effect of concrete, asphalt, and other artificial surfaces on heat waves. On the other hand, it is necessary to establish a

complete risk warning system, suitable disaster shelter planning, and a multilevel response mechanism. Appropriate urban planning strategies are particularly important for urban resilience and climate adaptation. In addition, a response strategy needs to be built for heat wave disasters for both prevention and control planning and emergency warning.

At present, the exploration of heat wave prevention, control, and management is still in its initial stage, and there is still a long way to go from theoretical research to strategy practice. In terms of research scale, this paper selects representative meteorological station data and mainly studies from the macro-regional level, while the data at the neighborhood level, which is directly related to urban residents, is still to be explored. The research and simulation of urban microclimate level data can help explore the impact of heat waves on buildings and the human body. In terms of an assessment system, a riskiness framework for heat wave risk assessment has been proposed in a related study. Subsequent studies will propose risk assessment factors for heat waves based on spatial and temporal characteristics analysis and establish a risk assessment system to provide a basis for developing more accurate and effective countermeasures.

Author Contributions: Conceptualization, H.H., Y.Y. and P.J.; methodology, H.H., P.J. and Y.Y.; software, P.J. and Y.Y.; validation, P.J.; formal analysis, P.J. and Y.Y.; investigation, H.H. and P.J.; resources, H.H.; data curation, P.J. and Y.Y.; writing—original draft preparation, P.J.; writing—review and editing, H.H. and S.M.; visualization, P.J.; supervision, H.H. and S.M.; project administration, H.H. and S.M.; funding acquisition, H.H. All authors have read and agreed to the published version of the manuscript.

Funding: This research was funded by the National Social Science Foundation of China: “Research on the Prevention, Control and Management Mechanism of Heat Wave Disasters in High-density Cities in Mountainous Areas, grant number 19BGL004; The National Natural Science Foundation of China: A typological approach and energy-saving potential of energy-saving renovation of existing residential buildings: A case study of Chongqing, grant number 52078071”.

Institutional Review Board Statement: Not applicable.

Informed Consent Statement: Not applicable.

Data Availability Statement: The data presented in this study are available on request from the corresponding author. The data are not publicly available due to privacy restrictions.

Acknowledgments: Thanks to fellow graduate students for providing technical support.

Conflicts of Interest: The authors declare no conflict of interest. The funders had no role in the design of the study; in the collection, analyses, or interpretation of data; in the writing of the manuscript, or in the decision to publish the results.

Nomenclature

IPCC	Intergovernmental Panel on Climate Change
PET	Physiological Equivalent Temperature
IHW	Intensity of Heat Waves
NHD	Number of Heat Wave Days
FHW	Frequency of Heat Waves
RCMs	Regional Climate Models
UHI	Urban Heat Island
CLC	Coastal Low Cloudiness
LST	Land Surface Temperature
VIIRS	Visible Infrared Imaging Radiometer Suite
DMSP	Defense Meteorological Satellite Program
EAHT	Effective Accumulated High Temperature
ARIMA	Autoregressive Integrated Moving Average
ACF	Autocorrelation Figure
PACF	Partial Autocorrelation Figure
USR	Urban Surface Roughness
UEL	Urban Ecological Land

References

1. Veal, A.J. Climate change 2021: The physical science basis, 6th report. *World Leis. J.* **2021**, *63*, 443–444. [[CrossRef](#)]
2. Walczykiewicz, T.; Filipiak, J. SWOT analysis of the Institute of Meteorology and Water Management—National Research Institute in the context of World Meteorological Organization Reform adopted during its 18th Congress. *Meteorol. Hydrol. Water Manag. Res. Oper. Appl.* **2020**, *8*, 5–11. [[CrossRef](#)]
3. Anderson, G.B.; Bell, M.L. Heat Waves in the United States: Mortality Risk during Heat Waves and Effect Modification by Heat Wave Characteristics in 43 U.S. Communities. *Environ. Health Perspect.* **2011**, *119*, 210–218. [[CrossRef](#)]
4. Shiva, J.S.; Chandler, D.G.; Kunkel, K.E. Localized Changes in Heat Wave Properties Across the United States. *Earth's Future* **2019**, *7*, 300–319. [[CrossRef](#)]
5. Allen, M.J.; Sheridan, S.C. Mortality risks during extreme temperature events (ETEs) using a distributed lag non-linear model. *Int. J. Biometeorol.* **2018**, *62*, 57–67. [[CrossRef](#)] [[PubMed](#)]
6. Linares, C.; Díaz, J.; Negev, M.; Martínez, G.S.; Debono, R.; Paz, S. Impacts of climate change on the public health of the Mediterranean Basin population—Current situation, projections, preparedness and adaptation. *Environ. Res.* **2020**, *182*, 109107. [[CrossRef](#)]
7. National Meteorological Center; Public Meteorological Service Center of China Meteorological Administration. *High-Temperature Heat Waves Rating. General Administration of Quality Supervision, Inspection and Quarantine of the People's Republic of China; China National Standardization Administration: Beijing, China, 2012; p. 8.*
8. Meehl, G.A.; Tebaldi, C. More Intense, More Frequent, and Longer Lasting Heat Waves in the 21st Century. *Science* **2004**, *305*, 994–997. [[CrossRef](#)] [[PubMed](#)]
9. Aubrecht, C.; Özceylan, D. Identification of heat risk patterns in the U.S. National Capital Region by integrating heat stress and related vulnerability. *Environ. Int.* **2013**, *56*, 65–77. [[CrossRef](#)]
10. Heo, S.; Bell, M.L.; Lee, J.-T. Comparison of health risks by heat wave definition: Applicability of wet-bulb globe temperature for heat wave criteria. *Environ. Res.* **2019**, *168*, 158–170. [[CrossRef](#)]
11. Pu, X.; Wang, T.J.; Huang, X.; Melas, D.; Zanis, P.; Papanastasiou, D.K.; Poupkou, A. Enhanced surface ozone during the heat wave of 2013 in Yangtze River Delta region, China. *Sci. Total Environ.* **2017**, *603*, 807–816. [[CrossRef](#)]
12. Huynen, M.; Martens, P.; Schram, D.; Weijenberg, M.P.; Kunst, A.E. The Impact of Heat Waves and Cold Spells on Mortality Rates in the Dutch Population. *Environ. Health Perspect.* **2001**, *109*, 463–470. [[CrossRef](#)] [[PubMed](#)]
13. Kalkstein, L.S.; Jamason, P.F.; Greene, J.S.; Libby, J.; Robinson, L. The Philadelphia Hot Weather-Health Watch/Warning System: Development and Application, Summer 1995. *Bull. Am. Meteorol. Soc.* **1996**, *77*, 1519–1528. [[CrossRef](#)]
14. Chen, M.; Geng, F.H.; Ma, L.M.; Zhou, W.D.; Shi, H.; Ma, J.H. Analysis of heat wave events in the Shanghai area in the last 138 years. *Highl. Meteorol.* **2013**, *32*, 2597–2607.
15. Yuan, C.; Adelia, A.S.; Mei, S.; He, W.; Li, X.-X.; Norford, L. Mitigating intensity of urban heat island by better understanding on urban morphology and anthropogenic heat dispersion. *Build. Environ.* **2020**, *176*, 106876. [[CrossRef](#)]
16. Bell, J.E.; Brown, C.L.; Conlon, K.; Herring, S.; Kunkel, K.E.; Lawrimore, J.; Lubler, G.; Schreck, C.; Smith, A.; Uejio, C. Changes in extreme events and the potential impacts on human health. *J. Air Waste Manag. Assoc.* **2018**, *68*, 265–287. [[CrossRef](#)] [[PubMed](#)]
17. Wilhelmi, O.V.; Purvis, K.L.; Harriss, R.C. Designing a Geospatial Information Infrastructure for Mitigation of Heat Wave Hazards in Urban Areas. *Nat. Hazards Rev.* **2004**, *5*, 147–158. [[CrossRef](#)]
18. Huang, H.; Jie, P. Research on the Characteristics of High-Temperature Heat Waves and Outdoor Thermal Comfort: A Typical Space in Chongqing Yuzhong District as an Example. *Buildings* **2022**, *12*, 625. [[CrossRef](#)]
19. Dian-Xiu, Y.; Ji-Fu, Y.; Zheng-Hong, C.; You-Fei, Z.; Rong-Jun, W. Spatial and Temporal Variations of Heat Waves in China from 1961 to 2010. *Adv. Clim. Chang. Res.* **2014**, *5*, 66–73. [[CrossRef](#)]
20. Hu, L.; Huang, G.; Qu, X. Spatial and temporal features of summer extreme temperature over China during 1960–2013. *Theor. Appl. Climatol.* **2017**, *128*, 821–833. [[CrossRef](#)]
21. Kuglitsch, F.G.; Toreti, A.; Xoplaki, E.; Della-Marta, P.M.; Zerefos, C.S.; Türkeş, M.; Luterbacher, J. Heat wave changes in the eastern Mediterranean since 1960. *Geophys. Res. Lett.* **2010**, *37*, L04802. [[CrossRef](#)]
22. Li, X.-X. Heat wave trends in Southeast Asia during 1979–2018: The impact of humidity. *Sci. Total Environ.* **2020**, *721*, 137664. [[CrossRef](#)] [[PubMed](#)]
23. Lhotka, O.; Kyselý, J. Spatial and temporal characteristics of heat waves over Central Europe in an ensemble of regional climate model simulations. *Clim. Dyn.* **2015**, *45*, 2351–2366. [[CrossRef](#)]
24. Liu, G.; Zhang, L.; He, B.; Jin, X.; Zhang, Q.; Razafindrabe, B.; You, H. Temporal changes in extreme high temperature, heat waves and relevant disasters in Nanjing metropolitan region, China. *Nat. Hazards* **2014**, *76*, 1415–1430. [[CrossRef](#)]
25. Tian, L.; Lu, J.; Li, Y.; Bu, D.; Liao, Y.; Wang, J. Temporal characteristics of urban heat island and its response to heat waves and energy consumption in the mountainous Chongqing, China. *Sustain. Cities Soc.* **2021**, *75*, 103260. [[CrossRef](#)]
26. Son, J.-Y.; Lee, J.-T.; Anderson, G.B.; Bell, M.L. The Impact of Heat Waves on Mortality in Seven Major Cities in Korea. *Environ. Health Perspect.* **2012**, *120*, 566–571. [[CrossRef](#)]
27. Zhang, K.; Li, Z.; Liu, J.; Liu, F.; Bai, J. Study on the spatial and temporal characteristics of high temperature heat wave in Hebei and its impact on industry and transportation. *Geogr. Geogr. Inf. Sci.* **2011**, *27*, 90–95.
28. Yang, Z.; Shanyou, Z.; Junwei, H.; Yi, L.; Jiamin, X.; Wen, D. Study on the spatial and temporal distribution of high temperature heat waves in Nanjing. *J. Geoinf. Sci.* **2018**, *20*, 1613–1621.

29. Dousset, B.; Gourmelon, F. Satellite multi-sensor data analysis of urban surface temperatures and landcover. *ISPRS J. Photogramm. Remote Sens.* **2003**, *58*, 43–54. [[CrossRef](#)]
30. Clemesha, R.E.S.; Guirguis, K.; Gershunov, A.; Small, I.J.; Tardy, A. California heat waves: Their spatial evolution, variation, and coastal modulation by low clouds. *Clim. Dyn.* **2018**, *50*, 4285–4301. [[CrossRef](#)]
31. Chen, T.-L.; Lin, H.; Chiu, Y.-H. Heat vulnerability and extreme heat risk at the metropolitan scale: A case study of Taipei metropolitan area, Taiwan. *Urban Clim.* **2022**, *41*, 101054. [[CrossRef](#)]
32. Kendall, M.G. *Rank Correlation Methods*; APA PsycNet: Washington, DC, USA, 1962.
33. Mann, H.B. Nonparametric tests against trend. *Econom. J. Econom. Soc.* **1945**, *13*, 245–259. [[CrossRef](#)]
34. Chen, Y.; Li, Y. An Inter-comparison of Three Heat Wave Types in China during 1961–2010: Observed Basic Features and Linear Trends. *Sci. Rep.* **2017**, *7*, srep45619. [[CrossRef](#)] [[PubMed](#)]
35. Li, K.; Amatus, G. Spatiotemporal changes of heat waves and extreme temperatures in the main cities of China from 1955 to 2014. *Nat. Hazards Earth Syst. Sci.* **2020**, *20*, 1889–1901. [[CrossRef](#)]
36. Xie, W.; Zhou, B.; You, Q.; Zhang, Y.; Ullah, S. Observed changes in heat waves with different severities in China during 1961–2015. *Theor. Appl. Climatol.* **2020**, *141*, 1529–1540. [[CrossRef](#)]
37. Li, L.; Zha, Y. Population exposure to extreme heat in China: Frequency, intensity, duration and temporal trends. *Sustain. Cities Soc.* **2020**, *60*, 102282. [[CrossRef](#)]
38. Wang, J.; Meng, B.; Pei, T.; Du, Y.; Zhang, J.; Chen, S.; Tian, B.; Zhi, G. Mapping the exposure and sensitivity to heat wave events in China's megacities. *Sci. Total Environ.* **2020**, *755*, 142734. [[CrossRef](#)] [[PubMed](#)]
39. Jiang, P.; Liu, X.; Zhu, H.; Li, Y. Features of Urban Heat Island in Mountainous Chongqing from a Dense Surface Monitoring Network. *Atmosphere* **2019**, *10*, 67. [[CrossRef](#)]
40. Lu, J.; Li, C.; Yu, C.; Jin, M.; Dong, S. Regression Analysis of the Relationship between Urban Heat Island Effect and Urban Canopy Characteristics in a Mountainous City, Chongqing. *Indoor Built Environ.* **2012**, *21*, 821–836. [[CrossRef](#)]
41. Ming, Y.; Liu, Y.; Liu, X. Spatial pattern of anthropogenic heat flux in monocentric and polycentric cities: The case of Chengdu and Chongqing. *Sustain. Cities Soc.* **2022**, *78*, 103628. [[CrossRef](#)]
42. Bingyan, C.; Weiguo, S.; Qu, G. Analysis of climate characteristics and circulation situation of summer high temperature in Chongqing area. *J. Southwest. Univ. (Nat. Sci. Ed.)* **2010**, *32*, 73–80. [[CrossRef](#)]
43. Xiaoran, L.; Bingyan, C.; Tianyu, Z.; Hao, Z.; Baogang, Y. Characterization of temperature change in Chongqing area in the last 46 years. *Highl. Mt. Meteorol. Res.* **2009**, *29*, 39–43.
44. Guo, Q.; Sun, W.; Cheng, B.; Duan, C. Climatic characteristics of high temperature weather and its circulation situation in Chongqing in the past 48 years. *Yangtze River Basin Resour. Environ.* **2009**, *18*, 52–59.
45. Guo, J.; Han, G.; Xie, Y.; Cai, Z.; Zhao, Y. Exploring the relationships between urban spatial form factors and land surface temperature in mountainous area: A case study in Chongqing city, China. *Sustain. Cities Soc.* **2020**, *61*, 102286. [[CrossRef](#)]
46. Zhou, X.; Chen, H. Impact of urbanization-related land use land cover changes and urban morphology changes on the urban heat island phenomenon. *Sci. Total Environ.* **2018**, *635*, 1467–1476. [[CrossRef](#)] [[PubMed](#)]
47. Feng, R.; Wang, F.; Wang, K.; Wang, H.; Li, L. Urban ecological land and natural-anthropogenic environment interactively drive surface urban heat island: An urban agglomeration-level study in China. *Environ. Int.* **2021**, *157*, 106857. [[CrossRef](#)]
48. Toparlar, Y.; Blocken, B.; Maiheu, B.; van Heijst, G. A review on the CFD analysis of urban microclimate. *Renew. Sustain. Energy Rev.* **2017**, *80*, 1613–1640. [[CrossRef](#)]
49. Stone, B.; Hess, J.J.; Frumkin, H. Urban form and extreme heat events: Are sprawling cities more vulnerable to climate change than compact cities? *Environ. Health Perspect.* **2010**, *118*, 1425–1428. [[CrossRef](#)]